AN OPTIMIZATION TOOL FOR THE DESIGN OF SSTO VEHICLES WITH COMBINED AIR-BREATHING/ROCKET PROPULSION

F. Serraglia
ESA – ESRIN, Rome, Italy

M. Valorani
Dipartimento di Meccanica e Aeronautica, University of Rome "La Sapienza", Rome, Italy

Introduction

The objective of this study is to introduce an optimization tool, developed at DMA/ University of Rome "La Sapienza", for the design of a single stage to orbit (SSTO) launcher equipped with a combined air-breathing/rocket propulsion system, that works in a direct insertion mission in a 400Km- equatorial, circular orbit, [3,4]. The adoption of the air-breathing propulsion system, with an high specific impulse, lowers the overall propellant consumption increasing the payload ratio and the empty weight, therefore, obtaining a greater robustness and adaptability of the entire system. The developed methodology, starting from a baseline mission profile and from an assigned reference configuration for the aircraft, defines the optimal design of the ascent trajectory together with the schedule of the propulsion systems, a preliminary sizing of the entire launcher and an estimate of the main subsystems masses.

The optimal solution is obtained by means of the definition of a finite number of design parameters affecting the vehicle's design as well as several trajectory constraints. For optimal design, it is intended the configuration yielding the largest mission payload.

A combined engine constitutes a propulsion system obtained by integrating different base motors so as to meet the propulsive requirement of a SSTO mission launcher along the whole flight path from takeoff to orbit insertion [1,3,4,8]. The mission is split in flight segments during which the vehicle is propelled by the propulsion subsystem most suited to the segment operative conditions. The air-breathing engine performance strongly depends on the prevailing flight conditions; thus, the best system performance is achieved only when the vehicle's aerodynamic, structures, propulsion are optimized concurrently with the ascent trajectory [10].

The article is organized in three sections; the first discusses the selection criteria for the identification of the vehicle's reference configuration; the second section is devoted to the definition of the strategy of ascent; the last section discusses the proposed optimization procedure and the analysis of the results.

Vehicle reference configuration

The vehicle's sizing proceeds from a reference "lifting body accelerator" configuration, NASA (1998) [3,4], as it appears in Fig.1 after some simplifications; from this reference geometry, an automatic iterative optimization procedure adjusts the overall vehicle's envelope in order to satisfy the volumetric requirement set by the effective propellant consumption; the geometrical adjustment is obtained by a simple linear scaling that preserves the volumetric ratios of the reference configuration.

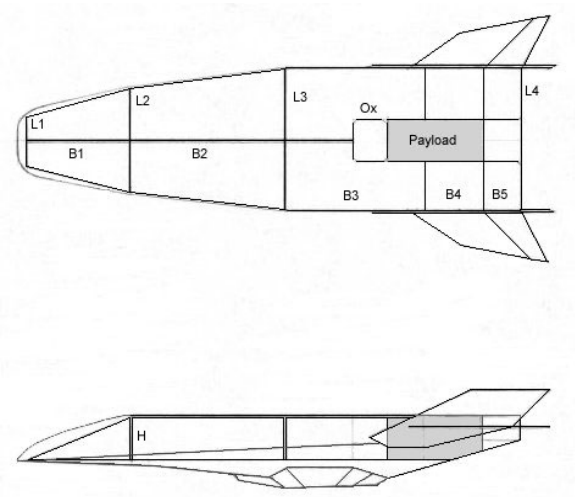

Fig. 1. Reference SSTO vehicle

The combined propulsion system comprises three different subsystems: the first operates at low speeds (turbo ramjet, 8 units), the second in the hypersonic regime (dual mode ramjet/scramjet, 3 units); both these two air-breathing engines employ liquid hydrogen as fuel. The third propulsion system is a liquid propellant rocket (LH_2/LO_X), which becomes operational outside the atmosphere and during orbital manoeuvres; it might also provide additional thrust across the transonic transition. The two air-breathing engines share a common variable-geometry inlet section as well as the rear inferior surface of the aircraft that acts as a plug, half-open, nozzle. The rocket engine is installed at the centre of the rear part of the aircraft, and it is equipped with a linear plug nozzle. The air-breathing engines inlet cross-sections as well as the throat section and the expansion ratio of the rocket engine are design parameters that need to be assigned through the optimization procedure.

The aerodynamic characteristics of the launcher as well as the performance of the entire air-breathing subsystem are made available as known functions of the instantaneous flight conditions: the aerodynamic coefficients, the thrust coefficient and the specific impulse are defined as functions of the flight Mach number, interpolating from data sets found in literature [1]. The performance of the rocket engine is calculated as a function of the flight conditions.

The model of the aircraft is completed with a module for the estimate of the weights of structures, tanks, propulsion subsystems, and thermal protections. The estimates here adopted have been extracted from statistical studies published in literature [5,6] as simple algebraic function of relevant design parameters.

Ascent strategy

During the atmospheric flight, the aircraft, propelled by the air-breathing subsystems, accelerates up to hypersonic speed (Mach > 10) in the upper layer of the stratosphere (Fig. 2); at even higher altitudes, the air-breathing system is switched off, this type of propulsion becoming less and less efficient, and the vehicle is propelled only by the rocket across the rarefied external bands of the atmosphere up to vacuum conditions.

The rocket engine extinguishes (burnout) once the vehicle reaches the conditions of insertion into an elliptic transfer orbit whose apogee attains the target orbit altitude; after the transfer coasting phase to the apogee point is completed, an impulsive ignition of the rocket engine finalizes the trajectory into the target circular orbit (strategy burn-coast-burn [7]).

The numerical integration of the equations of motion of the atmospheric flight is carried

out by following the variation in time of altitude, speed, angle of flight, range etc., from takeoff to burnout. The burnout condition detection, the characterization of the transfer orbit and the final circularization burn are determined analytically.

The specific form of the equations of motions here adopted is valid under the assumptions (*i*) of considering the aircraft as a variable-mass, material point and (*ii*) that the equilibrium of the motion around the centre of

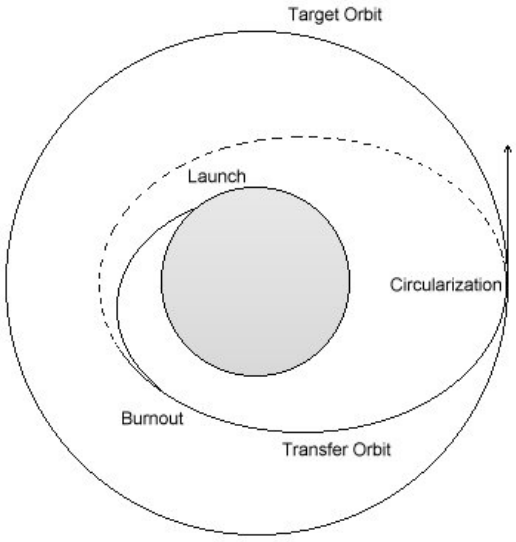

Fig. 2. SSTO Mission profile

mass is instantaneously satisfied. Flight conditions are assumed to be symmetrical with respect to the roll-axis, and all the acting forces are assumed to lie in the pitch-yaw plane; the flight path is completely equatorial and the Earth is considered to be perfectly spherical [1,8].

According to these hypotheses and to the notations of Fig. 3 the trajectory of the aircraft lies on the equatorial plane and can be found by solving numerically a set of four ordinary differential equations of the form:

$$\frac{\partial \vec{y}}{\partial t} = \vec{F}(\vec{y},\alpha,\varphi) \;\; ; \;\; \vec{y}(t=0) = \vec{y}_0 \qquad (1)$$

where the state vector is a vector valued function $\vec{y}[t] = (V[t],\gamma[t],h[t],x[t])$ collecting the following time varying variables: speed V, angle of the trajectory γ, altitude h, and range x; $\vec{F}[\vec{y}]$ defines an autonomous vector field. The equations of motion are parameterized with two control parameters: (*i*) the angle of attack α, and (*ii*) the thrust coefficient φ modulating the magnitude of the air-breathing subsystems thrust. Therefore, Eq. (1) is closed only when the rate laws of the two control parameters $\alpha(t)$ and $\varphi(t)$ are identified.

In general, the closure of Eq. (1) requires adding two more differential equations for $\alpha(t)$ and $\varphi(t)$.

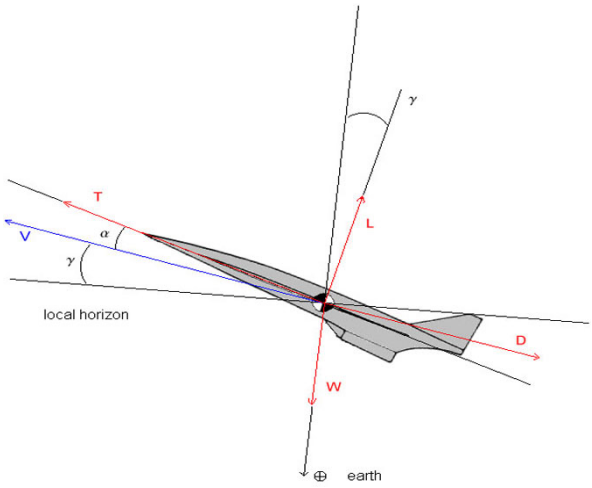

Fig. 3. Notations for the flight angles

However, under the assumption that the dynamical response of the vehicle to variations of the control parameters is instantaneous, allows replacing the two differential equations for $\alpha(t)$ and $\varphi(t)$ with two algebraic constraints expressing α and φ as function of the state variables only. The actual form of the algebraic constraints can be obtained once a control schedule is specified. In this work, we proceeded as follows. For what concerns the atmospheric flight, Fig. 4, the control strategy has been arranged in four phases:

Phase [1] *Initial Ascent* (A-A'): the aircraft, from a prescribed initial condition specified soon after takeoff – the takeoff details are not accounted for in the model - accelerates and rapidly gains altitude; we enforced a guidance law involving a constant growth rate of the angle of flight and an increase of the dynamic pressure towards some constant value, q_{cruise},

which is another optimization parameter; this guidance law affects both the angle of attack and the thrust modulation coefficient; φ keeps increasing along the flight path until it attains its limiting value of 1, at which instant the control strategy proceeds from phase 1 to 2.

Phase [2] *Cruise* (A'-C): during this phase of the atmospheric flight the control law prescribes the dynamic pressure to stay roughly constant at the value, q_{cruise}.

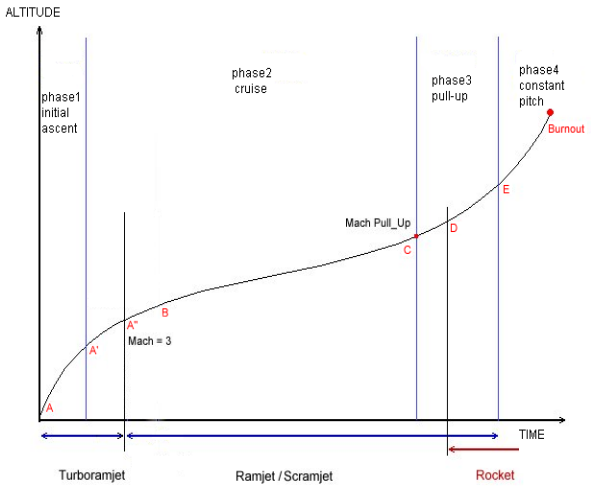

Fig.4. Control strategy

Crossing the flight Mach number of 3 triggers the transition from turbo ramjet to ram/scramjet propulsion [2]; the aircraft is controlled by acting on both control parameters. Again, the thrust modulation coefficient keeps increasing along the flight path and as soon as it saturates at its maximum the control law is enforced through variations of the angle of attack only. In this final trajectory segment, the aircraft operates in the hypersonic regime and is propelled by the scramjet subsystem. The Cruise phase terminates as soon as the flight Mach number reaches a certain value, M_{pull}, which is a further optimization. The flight phase that follows is the pull-up.

Phase [3] *Pull-up* (C-E): the aircraft, now in hypersonic flight along the trajectory in high atmosphere at a constant dynamic pressure (q_{cruise}), must necessarily gain altitude and speed in order to reach suitable orbit insertion conditions; a constant growth rate of the angle of flight is enforced through variations of the angle of attack. In the meantime, due to the increasing altitude and flight speed, the air-breathing propulsion system becomes less and less efficient, and at some point of the pull-up manoeuvre, the rocket engine must be ignited (point D). The exact moment of ignition is determined according to an appropriate design parameter, THR, to be optimized. Once the rocket is ignited, it operates in parallel with the scramjet until the air-breathing is definitively extinguished when its operative limits are reached (point E). The final shutdown of the air-breathing system initiates the last phase of the mission.

Phase [4] *Orbit Insertion* (E-Burnout): for this last phase of propelled flight, ending at the burnout condition, a constant pitch trajectory has been chosen, since it is well known that such a strategy maximizes, in first approximation, the burnout velocity. The control is carried out through variations of the angle of attack.

Optimization and results

The core of the optimization methodology is the evaluation of the flight trajectory obtained by means of the numerical integration of the equations of motion: during this procedure, the integrator continuously exchanges data and information with submodels built to represent the main aspects of the problem, such as propulsion, aerodynamics, control etc. and, through these, it is influenced by most of the design parameters introduced.

The flow-chart relative to the optimization procedure is shown in Fig. 5:

- First, an initial set of design parameters is tentatively assigned.
- Next, the equations of motion are integrated from a prescribed initial condition of the state variables, with a given takeoff gross weight and a first geometric sizing of the vehicle.

- Once a successful mission (one that reaches the burnout conditions without crashing) is found, that is once the atmospheric flight trajectory is fully identified, allows to evaluate the orbital maneuvers required to reach the target orbit.
- Weight and volume of the overall consumed propellant can now be calculated; starting from this information, the weight of all subsystems is evaluated as a function of the design parameters and the payload weight is finally obtained.
- At this point an iterative procedure is started in order to verify if the initial geometry is coherent with the one obtained as a function of the actual volumetric requirements found at the end of the mission; thus all the previous steps are repeated until convergence is achieved (*inner loop*).
- Once the geometrical convergence has been verified, the objective function and its gradient with respect to each of the design parameters are evaluated.
- The objective function and its gradient are passed as inputs to the optimization algorithm which verify if the optimum condition has been reached; if this is not the case, the design parameters are perturbed and another complete run is launched, (*main loop*).

The interaction among the several aspects of the system (aerodynamic, propulsion, weights and performances) is highly nonlinear and the optimal design solution can be far from being easily heuristically guessed, and nearly impossible to be obtained through a parametric analysis involving a single design parameter at time; the final configuration is going to be the best compromise among not singularly-optimal parameter definitions.

Although an unconstrained optimization procedure has been adopted, a preliminary sensitivity analysis has been carried out in order to define and characterize the range of variability of the different design parameters; moreover during the optimization loops several important aspects of the system not included directly as design parameters, such as load factors, maximum dynamic pressure, maximum angle of attack are constantly monitored to warn against extreme flight conditions. This way the optimization procedure can be safely initialized with computational time savings and avoidance of unfeasible solutions.

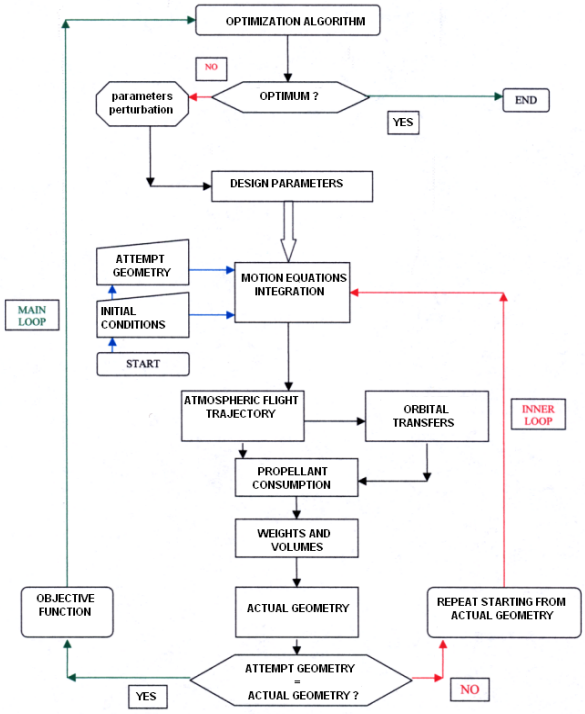

Fig. 5

The optimization algorithm adopted is based upon the Sequential Quadratic Programming (SQP) gradient method. The time-history of the objective function convergence is reported in Fig. 6, which shows that the payload is almost doubled with respect to the initial design. The optimal design results are reported in the Tab.1.

From Tab.1, we can observe that the duration of the optimized mission is 6800 s and therefore much longer than a typical ascent mission of a rocket-propelled launcher (~800s); the overall mission consists in an extended atmospheric flight (~4500s), and a ballistic phase

along the transfer orbit (~2260s) representing only one third of the total flight time.

The atmospheric flight, Fig. 7, is made of a long cruise phase, during which the vehicle, propelled by the combined air-breathing system, accelerates from Mach 2 up to Mach 15.

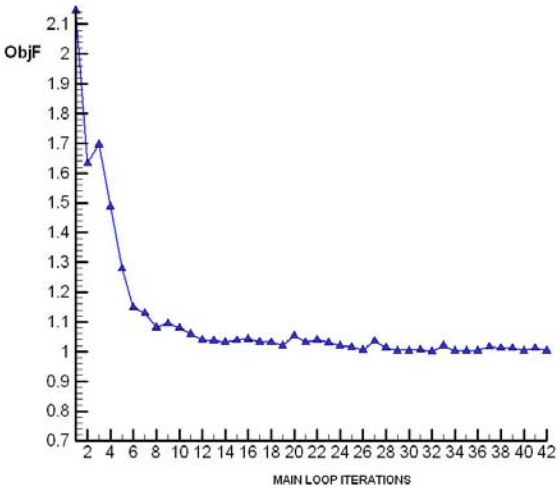

Fig.6. Convergence history of the objective function

REFERENCE MISSION		
Objective Orbit	400	(km)
Initial weight TOGW	416000	(kg)
DESIGN PARAMETERS		
Cruise dynamic pressure	90,000	(N/m^2)
Initial ascent angle variation	$1.18x10^{-3}$	(rad/s)
Pull-up angle variation	$1.02x10^{-5}$	(rad/s)
Pull-up Mach number	14.919	(-)
Rocket ignition parameter (THR)	27.277	(-)
Rocket expansion ratio	60.0	(-)
Rocket throat section	0.1	(m^2)
Turboramjet inlet section	6.578	(m^2)
Ram/scram inlet section	24.0	(m^2)

PERFORMANCES		
Payload	19214	(kg)
Total flight time	6775	(s)
Dry weight	115417	(kg)
Propellant consumption	275851	(kg)
Average specific impulse	699	(s)
Payload ratio	0.0461	(-)
Mass ratio	2.968	(-)
Structural ratio	0.294	(-)
Propellant ratio	0.663	(-)
Total; vehicle length	50.5	(m)

Table 1; Design parameters at the optimal design point.

Fig. 8 shows the time-history of the thrust as well as the optimal strategy adopted to manage the transition among the different propulsion sub-systems as well as the thrust obtained along the flight path.

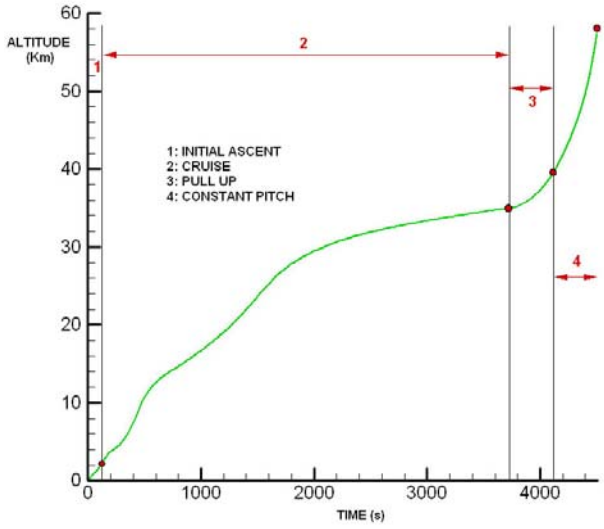

Fig.7. Details of the atmospheric flight

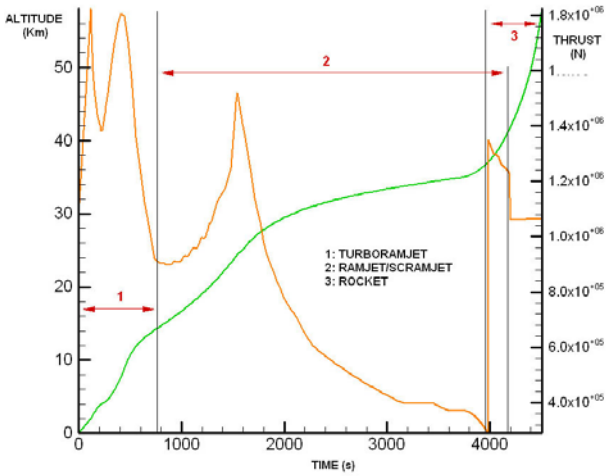

Fig.8. Altitude and thrust time histories of the atmospheric flight

The peak thrust values (Fig. 8) are found during the air-breathing system operation: a first maximum is obtained during the turbo ramjet operation (t = 150 s) when the thrust

modulation coefficient, according to the control requirements, reaches its maximum; then, a local minimum is recorded at t=300s followed by a second maximum at t=400s. This behaviour results from the opposite influence of the thrust coefficient $C_T(M)$, which diminishes with increasing flight Mach numbers, and the dynamic pressure which has to increase in order to attain the value prescribed by the control law. As soon as the turbo ramjet operative limit is reached (Mach=3), the dual-mode ramjet/scramjet system is ignited and the thrust is controlled by means of the modulation coefficient. Later, this engine is also pushed to its peak performance, this yielding a third thrust peak at about t=1600s; from this moment on, as the aircraft keeps accelerating and gaining altitude, the performance of the air-breathing system starts to decay because of the progressive rarefaction of the ingested airflow.

At this stage, the ignition of the rocket engine (Phase 3) gives the last impulse to reach the burnout conditions. Notice in Fig. 8, in-between t=4000s and 4200s, that the scramjet and the rocket engine are both operative.

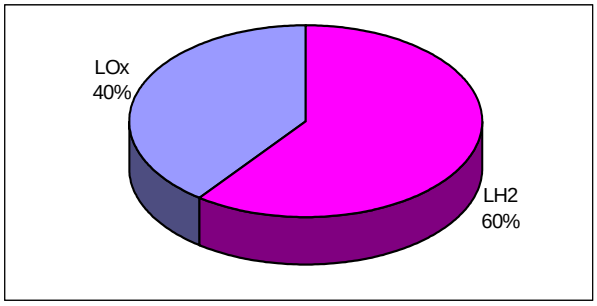

Fig.9. Propellant consumption in percent mass during atmospheric flight

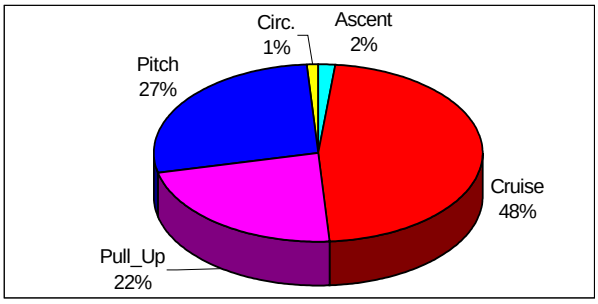

Fig.10. % Propellant consumption of each flight phase

During the long air-breathing propelled atmospheric flight 60% of the propellant consumption is made of LH2 (Fig. 9); this leaves to LOX a substantial 40% to be consumed during the relatively short rocket-propelled flight segment. Fig. 10 depicts how the propellant consumption is distributed among the flight segments; it is significant that the pull-up and the constant pitch phases consume 22% and 27% of the total consumption respectively, although they both have a much shorter duration than the cruise flight segment (48% of total consumption). Note that the rocket-based circularization manoeuvre absorbs a not negligible propellant amount (1% of total consumption).

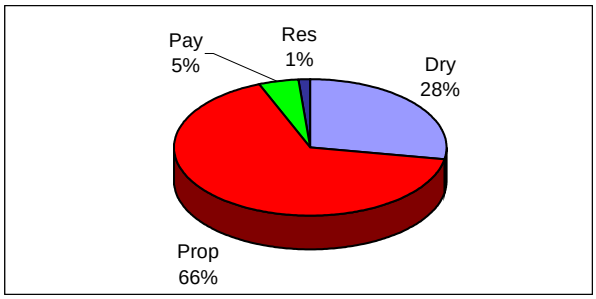

Fig.11. Takeoff gross weight distribution

Fig.11 reports the takeoff gross weight fraction; 66% of the total takeoff weight is made of propellants and tanks weights, while the dry weight represents nearly 30% of the total. The dry weight distribution among the subsystems is shown in Fig. 12: the contribution of structures (body + thermal protections, approximately 35 tons), tanks (approximately 40 tons) and motors (approximately 40 tons) is nearly equivalent. This particular dry weight

distribution is rather different from the one characterizing a traditional rocket propelled launcher where both the dry weight and the propulsion system take a much smaller fraction of the overall takeoff weight.

Conclusions

This work describes a design tool tailored for SSTO mission with a combined air-breathing/rocket propulsion system. The design tool involves the assembling of a number of modules built upon specific mathematical models for the definition of the flight trajectory from takeoff up to orbit insertion, a preliminary structural sizing of the launcher, an optimal control strategy and the estimation of the main subsystems weights. In particular, the optimal design defines the schedule of the transitions among the propulsion subsystems constituting the combined engine of the SSTO launcher.

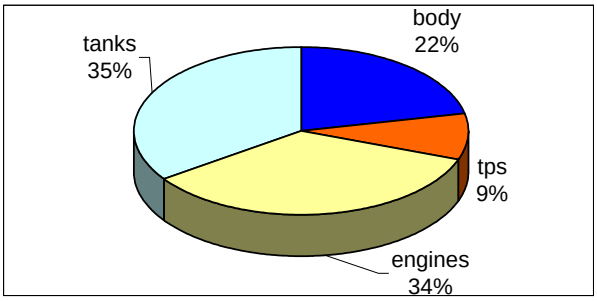

Fig.12. Dry weight distribution

A systematic parametric analysis and the comparison of the optimal design found with the recent literature findings [] suggest that the proposed design tool is capable of reproducing the main subsystem interactions.

Acknowledgements

The Italian Space Agency (ASI) and the Italian Ministry of Education, University and Research (MIUR) supported this work.

References

[1] H.G.Kauffman, R.V.Grandhi, W.L.Hankey, P.J.Belcher ; "Improved Airbreathing Launch Vehicle Performance with the Use of Rocket Propulsion". *Journal of Spacecraft* ,Vol. 28, No. 2. 1990.

[2] W.H.Reiser, D.D.Pratt ; "*Hypersonic Airbreathing Propulsion*". AIAA Education Series 1994.

[3] L.F.Scuderi, G.F.Orton, J.L.Hunt ; "Mach 10 Cruise/Space Access Veihicle Definition". Paper No.98-1584 *AIAA 8th Space Planes and Hypersonic Systems and Technologies Conference*, Norfolk, Va, Usa, April 27-30 1998.

[4] J.L.Hunt, V.L.Rausch ; "Airbreathing Hypersonic Systems Focus at NASA Langley Research Center". Paper No. 98-1641 *AIAA 8th Space Planes and Hypersonic Systems and Technologies Conference*, Norfolk, Va ,Usa, April 27-30 1998.

[5] G.J.Harloff, B.M.Berkowitz ; "*HASA-Hypersonic Aerospace Sizing Analysis for the Preliminary Design of Aerospace Vehicles*". NASA/CR-182226 Nov 1998.

[6] M.D.Ardema ; "*Body Weight of Hypersonic Aircraft*". NASA/TM-1998-101028.

[7] M.R.Goodel, W.C.Elrod ; "Suborbital Launch Trajectories for Satellite Delivery". *Journal of Spacecraft and Rockets*, Vol. 32, No. 3, May-June 1995.

[8] H.Tguchi, H.Futamura et al. ; "Conceptual Study of Pre-cooled Air Turbojet/Rocket Engine with Scramjet". *14th Symposium on Air Breathing Engines*, Florence, Italy, Sept. 5-10, 1999.

[9] G.P.Menees, H.G.Adelman, J.L.Cambier, J.V.Bowles ; "Wave Combustors for Trans-Atmospheric Vehicles". *Journal of Propulsion and Power*, Vol.8,No.3, May-June 1992.

[10] P.A.Czsyz ; "Combined Cycle Propulsion. Is it the key to achieving low payload to orbits costs ?". *14th Symposium on Air Breathing Engines*, Florence, Italy, Sept. 5-10, 1999.